Nanomaterials

DOI: 10.1002/anie.201004926

Excitation-Intensity-Dependent Color-Tunable Dual Emissions from Manganese-Doped CdS/ZnS Core/Shell Nanocrystals**

*Ou Chen, Daniel E. Shelby, Yongan Yang, Jiaqi Zhuang, Tie Wang, Chenggang Niu, Nicoló Omenetto, and Y. Charles Cao**

Manganese-doped semiconductor nanocrystals exhibit unique optical and magneto-optical properties, which make them excellent testbeds for both fundamental studies and technological applications in fields ranging from spintronics to biomedical diagnosis.[1–7] Large Zeeman effects have been observed in Mn-doped ZnS, ZnSe, and CdSe nanocrystals, which indicate that quantum-confined excitons feel a large effective magnetic field of up to 400 Tesla induced by the presence of a few Mn^{2+} ions inside the nanocrystals.[1,2] Spin-polarizable excitonic photoluminescence (PL) has also been observed in Mn-doped CdSe nanocrystals.[8,9] Additionally, Mn dopants can introduce new luminescence properties to nanocrystals, resulting in particles with dual emission properties.[1–11] Recent work has shown that Mn-doped CdS/ZnS core/shell nanocrystals possess dopant-position-dependent PL properties, and Mn dopants can be used as a radial pressure gauge for measuring the lattice strains in the nanocrystals.[12–14] Moreover, the PL from Mn dopants in Mn-doped ZnSe nanocrystals can be reversibly depleted by light-driven modulation using two excitation sources with different wavelengths.[15] Therefore, Mn-doped nanocrystals are a potential new class of optical microscopy markers that can improve optical imaging resolution in the far field.[15] Herein, we show that Mn-doped CdS/ZnS core/shell nanocrystals exhibit color-tunable dual emissions under a single-wavelength excitation source at varying intensities. This new finding provides important insight into the fundamental mechanisms of internal electronic transitions in Mn-doped semiconductor nanocrystals, which is important for applications such as photoswitchable markers for biomedical imaging and diagnosis.[16]

The PL properties of Mn-doped nanocrystals have been widely studied in the past two decades.[1–15,17] In general, when a photon is absorbed by a Mn-doped nanocrystal, an electron–hole pair (an exciton) is created and confined inside this nanocrystal.[3,17] This exciton can be deactivated via three pathways: 1) radiative recombination at the nanocrystal band edge, with the rate constant $k_{BE\text{-}R}$; 2) non-radiative recombination at the nanocrystal band edge, with the rate constant $k_{BE\text{-}NR}$; and 3) energy transfer to a Mn ion inside the nanocrystal, with the rate constant $n k_{ET}$, where n is the number of Mn ions doped inside one nanocrystal (Figure 1).

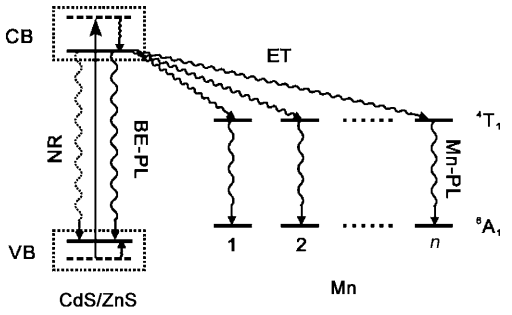

Figure 1. Energy levels and carrier relaxation pathways in a manganese-doped nanocrystal. CB conduction band, VB valence band, ET energy transfer, BE band edge, PL photoluminescence.

After the energy is transferred to a Mn ion, the excited Mn ion (at $^4T_1$) relaxes to its ground state ($^6A_1$) radiatively with the rate constant $k_{Mn\text{-}R}$, or nonradiatively with the rate constant $k_{Mn\text{-}NR}$. Under weak excitation,[17] the energy transfer efficiency (Φ_{ET}) and the spectrally integrated intensity ratio of the two emissions (I_{BE}/I_{Mn}) is expressed by Equations (1) and (2):

$$\Phi_{ET} = \frac{n k_{ET}}{k_{BE-R} + k_{BE-NR} + n k_{ET}} \quad (1)$$

$$\frac{I_{BE}}{I_{Mn}} \propto \left(\frac{k_{BE-R}}{n k_{ET}}\right) \frac{k_{Mn-R} + k_{Mn-NR}}{k_{Mn-R}} \quad (2)$$

Previous studies have shown that Φ_{ET} and I_{BE}/I_{Mn} are dependent on n, but not on the excitation intensity in the weak excitation regime (that is, less than one photon per nanocrystal).[17] However, Φ_{ET} and I_{BE}/I_{Mn} should also be dependent on the excitation intensity in the strong excitation regime. Because the Mn^{2+} emission lifetime is on the order of milliseconds,[18] additional excitation of a nanocrystal with one of the Mn ions already at its excited state is possible through sequential absorbance of photons from an excitation source with a sufficiently high intensity.[19] In other words, multiple Mn dopants inside a nanocrystal are pumped to their excited states (Figure 1). As a consequence, the number of Mn dopants at their ground state (n) decreases as excitation

[*] O. Chen, D. E. Shelby, Dr. Y. Yang, Dr. J. Zhuang, Dr. T. Wang, Dr. C. Niu, Prof. N. Omenetto, Prof. Y. C. Cao
Department of Chemistry, University of Florida
Gainesville, Florida 32611 (USA)
Fax: (+1) 352-392-0588
E-mail: cao@chem.ufl.edu

[**] We thank Prof. R. Jin for lifetime measurements. Y.C.C. acknowledges the NSF (DMR-0645520 Career Award) and ONR (N00014-06-1-0911) for support of this research. N.O. thanks the NSF (CHE 0822469) for support of this research.

Supporting information for this article is available on the WWW under http://dx.doi.org/10.1002/anie.201004926.

intensity increases, and thus Φ_{ET} and I_{Mn}/I_{BE} should show a dependence on excitation intensity. To explore this possibility, we studied the PL properties of Mn-doped CdS/ZnS core/shell nanocrystals by using a XeCl excimer laser as an excitation source.

Four types of Mn-doped core/shell nanocrystals were synthesized according to our previous method.[13,14] These nanocrystals have a core size of 3.1 nm and a shell thickness of 1.55 nm (ca. 4.8 monolayers (ML)). Mn dopants are at 1.6 ML in the ZnS shell and have an average of 2, 6, 12, and 15 Mn ions per dot, respectively.[20] Under weak excitation from a fluorometer (Fluorolog-3, Horiba Jobin Yvon, Irvine, CA), all of these Mn-doped nanocrystals have two emission bands at about 405 nm (band-edge emission) and about 595 nm (Mn^{2+} emission).[20] The nanocrystals doped with six Mn ions have a band-edge-emission with a lifetime of 5 ns and much slower Mn emissions, of which lifetimes can be fitted perfectly by two exponential decays with lifetimes of 0.9 ms (ca. 5.0%) and 7.1 ms (ca. 95%).[18,20]

In a typical experiment, a hexane solution of the nanocrystals doped with six Mn ions (2.16 μM) was excited by a XeCl excimer laser (30 ns pulses with a repetition rate of 6 Hz at 308 nm).[20] The excitation fluence was fine-tuned with a set of neutral density filters. The emissions from this nanocrystal solution were detected utilizing a spectrometer (Ocean Optics, with an integration time of 1 s) at 90° geometry. In this experiment, the time interval between laser pulses (ca. 166 ms) is much longer than the Mn emission lifetime; therefore, the integrated emissions from the nanocrystals are determined only by the pump fluence of single pulses. At a fluence of 0.13 mJ cm^{-2}, the nanocrystals exhibit a PL spectrum with an intensity ratio I_{BE}/I_{Mn} of 0.29, which is almost the same as that obtained using the fluorometer (Figure 2a). With the increase of fluence, both I_{BE} and I_{BE}/I_{Mn} monotonically increase (Figure 2a,b). This result demonstrates a characteristic property of the carrier relaxation dynamics of a nanocrystal with multiple Mn ions at their excited state ($^4T_1$). Before all of the Mn ions in this nanocrystal were excited, higher fluences coincided with higher numbers of Mn ions at their excited state and lower numbers of Mn ions at their ground state [n in Eq. (1) and (2)]. Therefore, in such carrier relaxation processes, more photons are generated from the band-edge pathway, and thus both I_{BE} and I_{BE}/I_{Mn} increase as excitation fluence increases. After all six of the Mn ions in the nanocrystal are excited, the increased excitation fluence leads to a larger I_{BE} and thus a larger I_{BE}/I_{Mn} because of the increased number of absorption and emission events.[19]

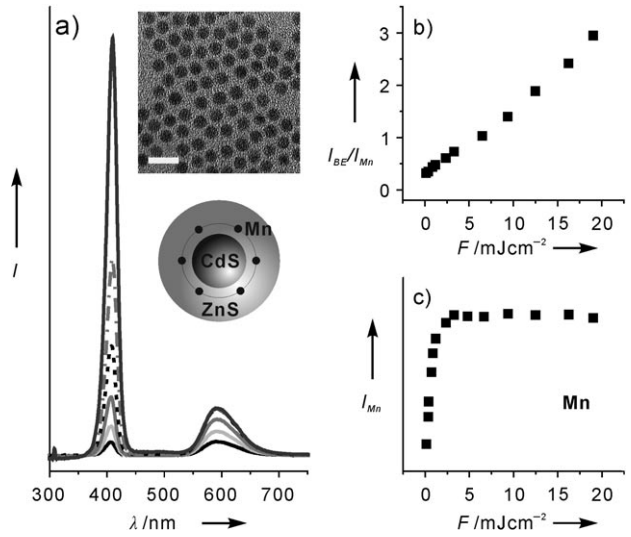

Figure 2. a) Photoluminescence spectra of CdS/ZnS core/shell nanocrystals doped with 6 Mn ions under a fluence of 0.13 to 19 mJ cm^{-2}.[20] Insets: a TEM image of these particles (scale bar 15 nm) and a cartoon of a Mn-doped core/shell particle. b) I_{BE}/I_{Mn} and c) I_{Mn} as a function of laser fluence.

The creation of a nanocrystal with multiple excited Mn ions is further confirmed by the result of the change in I_{Mn} (Figure 2c). With the increase of fluence, I_{Mn} increases and then reaches a maximum at the fluence of 3.3 mJ cm^{-2}. We attribute the increase of I_{Mn} to the increase of the number of Mn ions at $^4T_1$. This maximum Mn emission intensity is achieved because of the total excitation of all six Mn dopants in the nanocrystals (Figure 1). With a further increase of fluence, the maximum value of I_{Mn} remains nearly constant. This saturation of Mn emission intensity further suggests that all the Mn dopants inside individual nanocrystals are pumped to their excited state ($^4T_1$), and no more Mn dopants can accept the energy from the excitons of nanocrystals. In other words, the energy transition pathway from excitons to Mn dopants is closed under such excitation intensities, whereas the nanocrystal excitons can still relax to the ground state through the other two pathways: radiative recombination or non-radiative recombination at the nanocrystal band edge (Figure 1). Therefore, the further increase of band-edge emission intensity is allowed under excitation at a higher intensity, which is consistent with our measurements of I_{BE} and I_{BE}/I_{Mn} as a function of excitation fluence (Figure 2a,b). Furthermore, the excitation fluence for Mn emission reaching its maximum should depend on the number of Mn dopants inside a nanocrystal.

To test this possibility and further reveal the origin of excitation-intensity-dependent dual emissions, we also studied Mn-doped CdS/ZnS core/shell nanocrystals at different doping levels. The nanocrystals doped with 2, 12, or 15 Mn ions exhibit a similar PL property to that of those particles doped with six Mn ions (Figures 2, 3).[20] However, the Mn emission intensity of these particles reaches its maximum at different laser fluences (Figure 3). It is clear that the minimal fluence F_s required to saturate Mn emission is dependent on the average number of Mn ions inside a nanocrystal: $F_s =$ 1.3 mJ cm^{-2} for the particles with 2 Mn ions, 5.8 mJ cm^{-2} for the particles with 12 Mn ions, and 6.4 mJ cm^{-2} for the particles with 15 Mn ions (Figure 3d). These results further confirm that the saturation of Mn emission is a consequence of the total excitation of all of the Mn ions inside doped nanocrystals. Furthermore, these results suggest that the value of F_s can be used to semiquantitatively determine the doping level of Mn-doped nanocrystals.

To demonstrate the color-tunable property of the Mn-doped nanocrystals, we prepared a nanocrystal/polymer composite film, in which CdS/ZnS core/shell nanocrystals

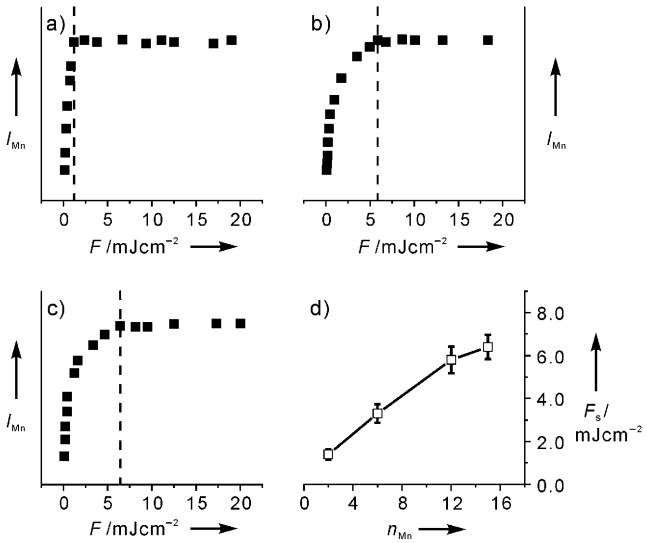

Figure 3. I_{Mn} as a function of laser fluence for the CdS/ZnS nanocrystals doped with a) 2 Mn ions, b) 12 Mn ions, and c) 15 Mn ions. d) F_s as a function of the average number of Mn ions n_{Mn} inside a dot.

doped with 20 Mn ions are used.[20] This film exhibits only Mn emission at 595 nm at a low excitation fluence (0.10 mJ cm^{-2}, Figure 4 a,d). By increasing the fluence to 2.7 mJ cm^{-2}, the emission at the nanocrystal band edge emerged, and the ratio between I_{BE} and I_{Mn} is 0.40. Because of the arising emission at the nanocrystal band edge, the color of the nanocrystal film changes from orange to purple (Figure 4 b,e). At an even higher fluence (60 mJ cm^{-2}), the ratio of I_{BE}/I_{Mn} increases to about 20, and the band-edge emission of the nanocrystals becomes the dominant radiative pathway. As a result, the nanocrystal film turns blue (Figure 4 c,f). This excitation-intensity-dependent color change is highly reversible. Amazingly, more than twenty thousand cycles of color switching between orange and blue have been recorded in the nanocrystal film (Figure 4 g). Observation of this extraordinary reversible and photoswitchable phenomenon is indebted primarily to the ultraphotostability of these Mn-doped CdS/ZnS nanocrystals. In contrast, we could not even observe the color-change effect at room temperature from Mn-doped ZnSe nanocrysals made by literature method, because these particles exhibit poor photostability under the strong excitation conditions used in this study.[20]

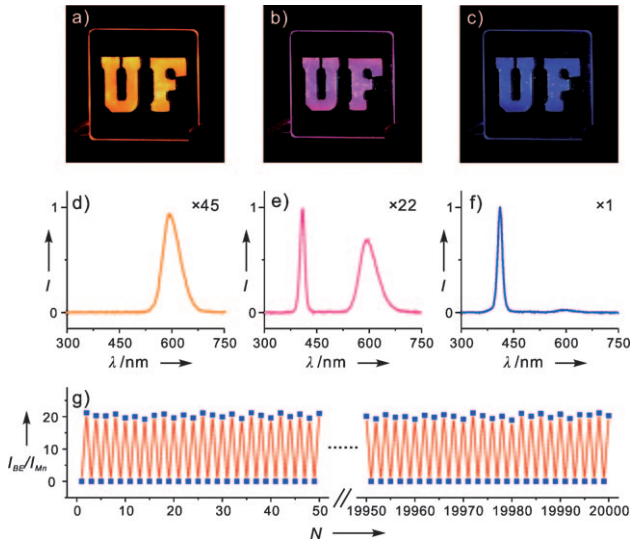

Figure 4. a–c) Optical images of a composite film of Mn-doped CdS/ZnS core/shell nanocrystals and polystyrene-*block*-polybutadiene under a fluence of a) 0.10, b) 2.7, and c) 60 mJ cm^{-2}. d–f) Corresponding PL spectra with normalized intensities. g) The color switching cycles (in counts N) of the nanocrystal film under two fluences (0.10 and 60 mJ cm^{-2}).

In conclusion, we present the first unambiguous evidence that Mn-doped semiconductor nanocrystals exhibit excitation-intensity-dependent dual emissions. The color-tunable property of these nanocrystals originates from the excitation of multiple Mn dopants inside a signal nanocrystal. Furthermore, we have discovered that the unique excitation fluence at which Mn-emission intensity reaches its maximum is dependent on the number of Mn dopants in a nanocrystal. Moreover, we have demonstrated that the color-tunable process in these nanocrystals exhibits extraordinary reversibility. We anticipate that the results herein would be useful for the design and synthesis of new functional nanomaterials with light-driven, color-tunable luminescence properties.

Experimental Section

Mn-doped CdS/ZnS core/shell nanocrystals were prepared according to a three-step synthesis method.[13,14] Briefly, in the first step, CdS/ZnS core/shell nanocrystals were synthesized with CdS core diameter of 3.1 nm and a ZnS shell of 1.6 ML by the typical core/shell growth method.[13,14] In the second step (dopant growth), a hexane solution of resulting core/shell particles (2 mL, 50.4 nmol) was added into a mixture solution of ODE (octadecene) and OAm (oleylamine) (8.0 mL, ODE/OAm: 3:1), and then hexane was removed under vacuum. Under an argon flow, the CdS/ZnS core/shell nanocrystal solution was heated to 280 °C, and then a $Mn(OAc)_2$ solution and sulfur solution ($Mn(OAc)_2$ and sulfur at a molar ratio of 1:1) were alternatively introduced into the hot solution by dropwise addition. The doping level was controlled by adding different amount of $Mn(OAc)_2$ and sulfur solutions. The synthesis was stopped after 20 min reaction. In the third step, the resulting CdS/ZnS core/shell nanocrystals with Mn dopants at surface was further overcoated with ZnS shell through alternate injections of the solutions of zinc stearate in ODE (40 mM) and sulfur in ODE (40 mM). Growth time was 10 min after each injection. Importantly, when the desired shell thickness (3.2 ML) was achieved, a large excess of zinc stearate (0.12 mmol) in ODE solution was injected into the reaction system. After 25 min, 1 mL of oleic acid was introduced into the solution and the synthesis was stopped by cooling the reaction solution to room temperature. The resulting nanocrystals were isolated by adding acetone and further purified by three precipitation–redispersion cycles using methanol and toluene. Final particles were dispersed in hexane.

Nanocrystals/polymer composite films were prepared by dissolving about 300 mg polystyrene-*block*-polybutadiene in a toluene solution with Mn-doped CdS/ZnS core/shell nanocrystals (1 mL, 1.08 μM), and aged overnight. After forming the high-viscosity homogenous solution, the solution was drop-casted onto a premade stencil with letters "U" and "F". After the toluene was totally evaporated away, the nanocrystal/polymer composite thin film was peeled off the stencil, and placed onto a quartz substrate (2.5 cm × 2.5 cm). This substrate was mounted and optically excited with the

output of a XeCl excimer laser (308 nm, pulse width of about 30 ns, repetition frequency of 6 Hz). The excitation fluence was controlled using a set of neutral density filters. Photoluminescence signals were collected by an optical fiber and detected using a spectrometer (SD2000, Ocean Optics) with an integration time of 1 s. The photographic images were taken with a digital camera (Canon EOS 40D).

Received: August 6, 2010
Published online: November 25, 2010

Keywords: doping · dual emission · nanomaterials · nanotechnology · photochemistry

[1] M. Shim, C. Wang, D. J. Norris, P. Guyot-Sionnest, *MRS Bull.* **2001**, 1005.
[2] J. D. Bryan, D. R. Gamelin, *Prog. Inorg. Chem.* **2005**, *54*, 47.
[3] D. J. Norris, A. L. Efros, S. C. Erwin, *Science* **2008**, *319*, 1776.
[4] D. Magana, S. C. Perera, A. G. Harter, N. S. Dalal, G. F. Strouse, *J. Am. Chem. Soc.* **2006**, *128*, 2931.
[5] N. Pradhan, D. Goorskey, J. Thessing, X. Peng, *J. Am. Chem. Soc.* **2005**, *127*, 17586.
[6] D. J. Norris, N. Yao, F. T. Charnock, T. A. Kennedy, *Nano Lett.* **2001**, *1*, 3.
[7] A. Nag, S. Chakraborty, D. D. Sarma, *J. Am. Chem. Soc.* **2008**, *130*, 10605.
[8] R. Beaulac, L. Schneider, P. I. Archer, G. Bacher, G. R. Gamelin, *Science* **2009**, *325*, 973.
[9] R. Beaulac, P. I. Archer, X. Liu, S. Lee, G. M. Salley, M. Dobrowolska, J. K. Furdyna, D. R. Gamelin, *Nano Lett.* **2008**, *8*, 1197.
[10] S. C. Erwin, L. Zu, M. I. Haftel, A. L. Efros, T. A. Kennedy, D. J. Norris, *Nature* **2005**, *436*, 91.
[11] H. Yang, P. H. Holloway, *Adv. Funct. Mater.* **2004**, *14*, 152.
[12] S. Ithurria, P. Guyot-Sionnest, B. Mahler, B. Dubertret, *Phys. Rev. Lett.* **2007**, *99*, 265501.
[13] Y. A. Yang, O. Chen, A. Angerhofer, Y. C. Cao, *J. Am. Chem. Soc.* **2006**, *128*, 12428.
[14] Y. A. Yang, O. Chen, A. Angerhofer, Y. C. Cao, *J. Am. Chem. Soc.* **2008**, *130*, 15649.
[15] S. E. Irvine, T. Staudt, E. Rittweger, J. Engelhardt, S. W. Hell, *Angew. Chem.* **2008**, *120*, 2725; *Angew. Chem. Int. Ed.* **2008**, *47*, 2685.
[16] S. W. Hell, *Science* **2007**, *316*, 1153.
[17] Y. A. Yang, O. Chen, A. Angerhofer, Y. C. Cao, *Chem. Eur. J.* **2009**, *15*, 1386.
[18] A. Ishizumi, E. Jojima, A. Yamamoto, Y. Kanemitsu, *J. Phys. Soc. Jpn.* **2008**, *77*, 053705.
[19] D. Oron, M. Kazes, I. Shweky, U. Banin, *Phys. Rev. B* **2006**, *74*, 115333.
[20] See the Supporting Information.

